Journal of Nuclear Materials 398 (2010) 109–115

Contents lists available at ScienceDirect

Journal of Nuclear Materials

journal homepage: www.elsevier.com/locate/jnucmat

Oxidation behaviour of P122 and a 9Cr–2W ODS steel at 550 °C in oxygen-containing flowing lead–bismuth eutectic

C. Schroer [a,*], J. Konys [a], T. Furukawa [b], K. Aoto [b]

[a] Karlsruhe Research Centre, Institute for Materials Research III, Hermann-von-Helmholtz-Platz 1, 76344 Eggenstein-Leopoldshafen, Germany
[b] Japan Atomic Energy Agency, O-arai Research and Development Center, 4002 Narita, O-arai, Ibaraki 311-1393, Japan

A B S T R A C T

The long-term performance of 12Cr–2W ferritic/martensitic steel P122 and a 9Cr–2W ODS steel was tested in oxygen-containing flowing lead–bismuth eutectic (LBE) at 550 °C and a flow velocity of 2 m/s by means of exposure experiments in the CORRIDA loop. The target for the enrichment of dissolved oxygen was a concentration, c_O, of 10^{-6} mass%, corresponding to a lead oxide (PbO) activity of approximately 10^{-3}. Owing to initial problems controlling c_O, some of the exposed specimens experienced varying conditions, which allowed for investigating the influence of temporarily low c_O (down to $\sim 10^{-9}$ mass%), in addition to constantly high c_O (averaging 1.6×10^{-6} mass%). Maximum exposure times at constantly high c_O were 10,000 and 20,000 h for P122 and the ODS steel, respectively. Under the testing conditions, both steels were affected by moderate oxidation resulting in the formation of a compact layer of a spinel-type oxide on the surface and a more or less pronounced internal oxidation zone. The thickness of the oxide scale was quantified and used for determining the material loss (metal recession). For $c_O \approx 10^{-6}$ mass%, logarithmic and power rate laws were fitted to the obtained data as a basis for predicting the metal recession at times exceeding the experimental exposure times. Temporarily lower c_O proved to be beneficial for the performance of both steels, while, in the case of the ODS steel, excursions to higher c_O should be prevented in order to achieve optimum oxidation resistance.

1. Introduction

For the use of liquid lead (Pb) or lead–bismuth eutectic (LBE) as a coolant and source of spallation neutrons in accelerator driven systems (ADS), the compatibility of these liquid metals with steels—the favoured construction materials for such plants—is of significant importance. In the absence of oxygen, the major steel constituents iron (Fe), chromium (Cr) and especially nickel (Ni) are prone to dissolution, which, depending on the temperature, may result in an unacceptably high rate of material degradation. In the case of flowing liquid metal with temperature gradients, steel constituents dissolved at high temperatures re-precipitate at low temperatures, giving rise to plugging of narrow flow paths. With increasing concentration of oxygen dissolved in liquid Pb or LBE, the mechanism of material degradation changes from dissolving corrosion to oxidation, accompanied by the formation of an oxide scale on the steel surface. If a continuous, non-porous oxide scale forms, dissolution of steel constituents can occur only after diffusion through the oxide scale, i.e., at a considerably reduced rate. Additionally, the presence of oxygen lowers the solubility of the scale-forming steel constituents, as follows from the solubility product of the respective oxides. For both liquid Pb and LBE, the theoretical upper limit for the enrichment of (dissolved) oxygen is determined by the precipitation of lead oxide (PbO) at the lowest temperature to be considered. In practice, the upper limit is determined by the oxidation rate of the employed steels which increases with increasing oxygen content of the liquid metal.

According to recent design studies on the implementation of an ADS for the transmutation of minor actinides in nuclear waste, parts of the thermally high-loaded fuel cladding and heat exchanger experience temperatures in the range from about 500–550 °C, which is well within the application limit of ferritic/martensitic (F/M) steels. Additionally, the expected behaviour of this class of steels under irradiation in the ADS is promising in comparison to austenitic steels, especially in the case of oxide-dispersion-strengthened (ODS) F/M steels produced by a powder metallurgic process. Although the operating temperatures intended for lead-cooled fast reactors (LFR) are somewhat higher, the performance of F/M steels under "ADS conditions" is also useful for the development of the LFR, one of the concepts pursued with respect to the fourth generation of nuclear power plants.

The increased demand for data on the behaviour of steels in the presence of liquid Pb and LBE is reflected by the numerous studies

* Corresponding author. Tel.: +49 (0)7247 82 4840; fax: +49 (0)7247 82 3956.
E-mail address: carsten.schroer@imf.fzk.de (C. Schroer).

0022-3115/$ - see front matter © 2009 Elsevier B.V. All rights reserved.
doi:10.1016/j.jnucmat.2009.10.019

on this subject reported in the technical literature during the last decade. In most of these investigations, LBE was employed at temperatures between 300 °C and 600 °C and concentrations of dissolved oxygen ranging from 10^{-10} mass% to oxygen saturation at the testing temperatures applied. An overview of the parameters in these tests which were conducted both in stagnant (crucible test) and flowing LBE (loop experiments), and a basic characterization of the performance of F/M and austenitic steels is given by Soler Crespo [1], along with the parameters and results of the comparatively few tests in stagnant or flowing liquid Pb. Another review concentrating on the performance of steels in LBE was publicized by Zhang and Li [2]. Considering these reviews (covering publications before 2006) and results of investigations reported more recently, there is a lack of data from loop experiments lasting $\geqslant$10,000 h that allow a (more) reliable quantitative assessment of the long-term performance of the different types of steels in flowing liquid Pb or LBE.

As candidate materials for the fuel cladding and heat exchanger in nuclear plants using Pb or LBE as a spallation target and/or coolant, the F/M steel P122, containing nominally 12 mass% Cr and 2 mass% tungsten (W), and a 9Cr–2W ODS steel (referred to as ODS in the following) were tested in oxygen-containing flowing LBE at 550 °C and a flow velocity, v, of 2 m/s. The target for the enrichment of oxygen in the LBE was an oxygen concentration, c_O, of 10^{-6} mass%, corresponding to an activity of PbO, a_{PbO}, of approximately 10^{-3}. Owing to initial problems controlling the oxygen content in flowing LBE, some of the specimens exposed experienced varying conditions with respect to the oxygen content, which allowed investigating the influence of temporarily low c_O (down to $\sim10^{-9}$ mass%), in addition to the performance at constantly high c_O ($\sim10^{-6}$ mass%). Maximum exposure times at constantly high oxygen content were 10,000 and 20,000 h for P122 and ODS, respectively.

2. Experimental

2.1. Sample material and specimen preparation

The chemical composition and heat-treatment parameters of the P122 and ODS samples employed are summarized in Table 1. Differences in the composition of the two steels that can be decisive for the performance in oxygen-containing LBE are the higher Cr content of P122—beneficial with respect to the stability of slow-growing Cr-rich oxides—and the small amounts of yttria (Y_2O_3) and titanium (Ti) in ODS which give rise to the presence of nano-scale particles of Y_2O_3 or yttrium (Y)–Ti mixed oxides dispersed in the microstructure of ODS [3]. Oxides dispersed in the steel can promote the nucleation of other oxides, e.g., those oxides that are capable of forming a protective scale on the steel surface, the more so the finer and homogeneous the dispersion. When characterizing the initial (as-received) state of ODS using scanning electron microscopy (SEM) supplemented by qualitative energy-dispersive X-ray micro-analyses (EDX), Ti-rich oxidic particles with a size between 0.2 and >1 μm were identified (*cf.* Fig. 11). Another potentially decisive difference between P122 and ODS is the exceptionally fine-grained martensitic structure of ODS (Fig. 1) resulting from a significantly retarded growth of austenite grains during normalization of the steel [3], and providing a high number of paths for fast diffusion of oxide forming steel constituents.

From the samples of P122 and ODS, cylinders with dimensions of ⌀8 × 35 mm were cut and provided with an internal and external screw-thread at the top and bottom end, respectively. The threads allow a number of these specimens to be joined and exposed simultaneously in the testing facility. The surface of the specimens was finished by turning and cleaned with acetone before exposure to oxygen-containing flowing LBE.

2.2. Testing conditions

Specimens of P122 and ODS were exposed to oxygen-containing flowing LBE in the CORRIDA loop (described in detail in [4]) at 550 °C (+5 °C) and v = 2 m/s (±0.2 m/s). Oxygen consumed by oxidation of the exposed specimens and the walls of the loop was replenished via transfer from a gas with adjustable oxygen partial pressure, and the oxygen content maintained in the LBE was continuously measured using electrochemical oxygen sensors in different positions along the loop. The chart of the electromotive force (E.M.F.) indicated by a platinum (Pt)/air sensor that is positioned at the inlet of the first test-section of the loop—where the specimens reside during the exposure—is shown in Fig. 2, along with c_O and the average a_{PbO} calculated from the sensor output [5]. During the first 5000 h of effective operation of the loop, distinct and comparatively long-lasting deviations of the indicated E.M.F. from the target value occurred, resulting from initial problems maintaining the desired oxygen level ($c_O = 10^{-6}$ mass%) in the flowing LBE. After improving the control of the oxygen content [4], the E.M.F. fluctuated for short periods, but mostly was in a narrow range around the target value for the remaining 25,000 h of the total runtime of the exposure experiment. In this interval, the average c_O was 1.6×10^{-6} mass%, corresponding to $a_{PbO} \approx 10^{-3}$. Considering the formation of Fe–Cr oxides on the surface of P122 and ODS, chromia (Cr_2O_3) and Fe–Cr spinel ($FeCr_2O_4$) were always stable under the conditions of the exposure experiment, while magnetite (Fe_3O_4) was temporarily unstable between ~2800 and 3700 h of effective operation of the loop. The exact exposure times and intervals for the specimens of P122 and ODS are listed in Table 2, together with a brief summary of the conditions with respect to the oxygen content of the LBE that follow from Fig. 2.

2.3. Post-test examinations

For each exposure time, two half-cylindrical pieces of approximately 10 mm length and a circular slice of 2–3 mm thickness were cut from the cylindrical specimens in the condition as taken from the loop. One of the half-cylindrical pieces and the circular slice were used to prepare a longitudinal and vertical cross-section, respectively. Both cross-sections were inspected using light-optical

Table 1
Chemical composition (in mass%) and heat-treatment parameters for the samples of P122 and ODS from which the specimens for the exposure experiments were machined.

P122											
Fe	Cr	W	Cu	Mn	Mo	Ni	Si	V	Nb	C	N
Bal.	10.54	1.72	1.00	0.64	0.34	0.33	0.27	0.19	0.048	0.11	0.071
Final heat treatment (massive block with a thickness of ~200 mm): 100 min at 1070 °C (air cooling [AC]) + 400 min at 770 °C (AC)											
ODS											
Fe	Cr	W	Y	Ti	O	C	N				
Bal.	8.85	1.94	0.27	0.20	0.17	0.13	0.011				
Final heat treatment (cylindrical bar with ⌀10 mm): 60 min at 1050 °C (AC) + 60 min at 800 °C (AC)											

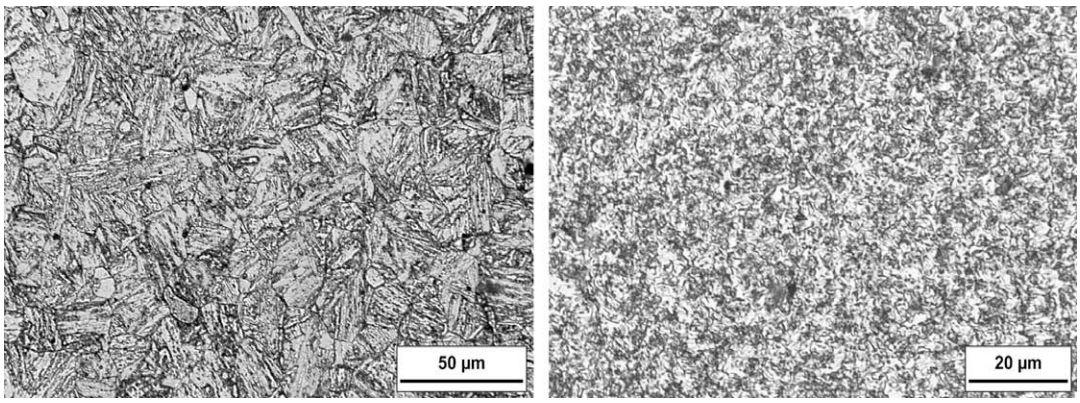

Fig. 1. Martensitic microstructure of P122 (left) and ODS (right) in the as-received state of the samples. Note the higher magnification of the right micrograph.

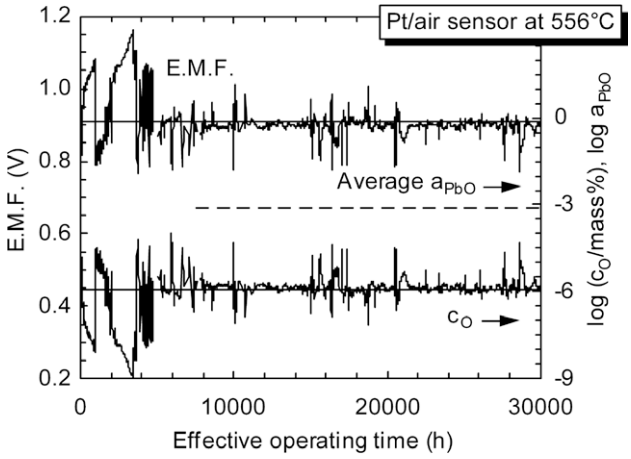

Fig. 2. E.M.F. indicated by the Pt/air sensor at the inlet of the first test-section of the CORRIDA loop, calculated c_O and average a_{PbO} (dashed line) as a function of the effective operating time of the loop.

microscopy (LM). Subsequently, at least the vertical cross-section was examined in the SEM supplemented by qualitative EDX analyses. In the case of the specimens of P122 and ODS that were exposed for 2018 h, the composition of corrosion products (oxides) formed on the surface of the steels were quantitatively assessed by means of electron-probe micro-analysis (EPMA). A phase analyses of the corrosion scale on P122 and ODS by X-ray diffraction (XRD) was performed using the second half-cylindrical piece of the specimens that were exposed for 4990 h, after stripping off adherent LBE in hot fat at ~160 °C. For quantifying the corrosion damage, the thickness of the distinguishable parts of the corrosion scales were measured in the LM using the vertical cross-section of the specimens after exposure; generally, 12 positions uniformly distributed along the specimen circumference were analysed. The loss of material with sound properties (metal recession) was determined indirectly from the observed corrosion scale [4,6].

3. Results and discussion

3.1. P122

Characteristic for the performance of P122 in oxygen-containing flowing LBE at 550 °C and $v = 2$ m/s, irrespective of whether c_O was constantly around 10^{-6} mass% or varied considerably between higher and much lower values, is the initial presence of a thin Cr-rich oxide scale (<1 µm) that is successively replaced by an Fe–Cr mixed oxide, resulting in a piecewise continuous layer of non-uniform thickness (Fig. 3). XRD and EPMA analyses of this oxide indicate a Cr-deficient Fe–Cr spinel, $Fe(Fe_xCr_{1-x})_2O_4$. Generally, an internal oxidation zone (IOZ) develops beneath the spinel. The IOZ consists of a Cr-rich oxide (a Cr-rich spinel, Cr_2O_3 or a mixed oxide based on Cr_2O_3) dispersed in the Cr-depleted steel matrix. However, an IOZ can locally be missing, especially where a comparatively thin spinel layer formed. Regardless of whether or not an IOZ is present, the steel at the interface with the oxide scale is slightly depleted in Cr, up to a depth of 2–4 µm after 10,000 h. Copper (Cu) which accounts for 1 mass% of the steel was found in the form of metallic particles dispersed in the spinel. Considering exposure times ⩾5000 h, intermittently very low oxygen content decreases the share of internal oxidation in the oxide scale, which was especially pronounced for the specimen of P122 that resided in the loop in the interval from 0 to 5016 h of total runtime of the experiment. In the case of this specific specimen, an IOZ was mostly missing and, if present, thin in comparison to the average IOZ developed at constantly high c_O after comparable exposure time. Qualitative EDX analyses revealed a significant accumulation of Cr in the spinel at the spinel/steel interface in the absence of an IOZ. According to the post-test examination of the P122 specimen that was exposed in the interval from 0 to 10,006 h, this accumulation of Cr in the inner part of the spinel partially persists during following periods of constantly high c_O.

The evolution of the average thickness of the Fe–Cr spinel and IOZ with time at constantly high c_O is depicted in Fig. 4. Only sites where apparently all the spinel that was formed in the course of the exposure to oxygen-containing LBE adhered to the specimen—which, as discussed below, was not always the case—were regarded when performing the respective measurements in the LM. Data obtained from a parallel study on welded P122 that experienced a different heat treatment before the exposure is included in this figure, so as to approximate the oxide-scale growth at constantly high c_O for exposure times ⩽2000 h. For evaluating the trend in the evolution of the two parts of the oxide scale, power, (direct) logarithmic and inverse logarithmic functions of time were considered [7], with comparably good results for the power and logarithmic functions (Fig. 4 exhibits the respective logarithmic curves). According to Fig. 4, the main part of the oxide scale on P122 is Fe–Cr spinel and the importance of internal oxidation only slightly decreases with increasing time at constantly high c_O. During periods of very low c_O, the share of internal oxidation decreases more significantly in concurrence with the accumulation of Cr at the inner interface of the spinel. Assuming that, in the absence of partial detachment, the surface of the spinel approximately coincides with the original steel surface, the metal recession can be estimated from the sum of the thickness of spinel and IOZ [4,6]. The results are depicted in Fig. 5, both for constantly high and

Table 2
Summary of exposure times and intervals and conditions with respect to the oxygen content for P122 and ODS in the CORRIDA loop (LBE/550 °C/2 m/s).

Exposure time (h)	Exposure interval (h)	c_O (mass%)	
818	0–818	10^{-8}–10^{-5}	Exposure started with high c_O, followed by a rapid decrease
2018	0–2018	10^{-8}–3×10^{-5}	Long-term fluctuation between high and low c_O
5016	0–5016	10^{-9}–3×10^{-5}	c_O below threshold for Fe_3O_4 stability in the middle of the interval, short-term fluctuations at the end
10,006	0–10,006	10^{-9}–3×10^{-5}	c_O mostly around 10^{-6} mass% in the second half of the interval
4990	5016–10,006	3×10^{-7}–3×10^{-5}	Fluctuations of c_O around 10^{-6} mass%, $c_O > 10^{-6}$ mass% in the beginning
5011	10,006–15,017	3×10^{-7}–3×10^{-5}	Fluctuations of c_O around 10^{-6} mass%, $c_O \leqslant 10^{-6}$ mass% in the beginning
10,001	5016–15,017	3×10^{-7}–3×10^{-5}	See interval 5016–10,006 h
20,039[a]	10,006–30,045	3×10^{-7}–3×10^{-5}	See interval 10,006–15,017 h

[a] Only ODS.

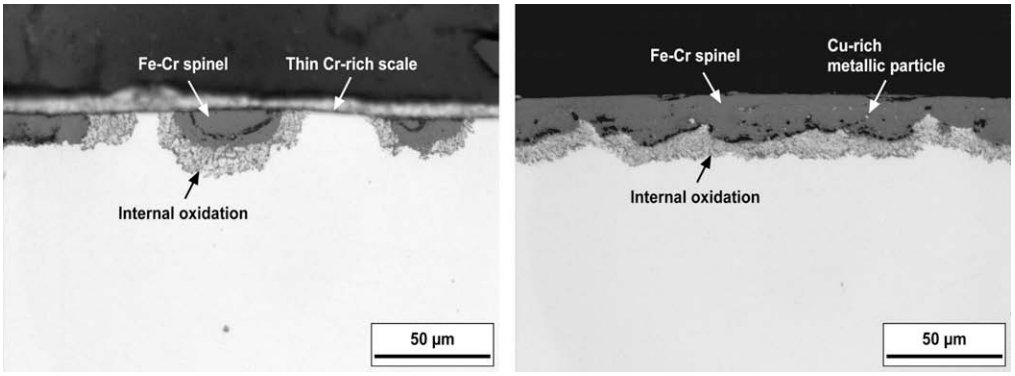

Fig. 3. Oxides on the surface of P122 formed in flowing LBE at 550 °C and constantly high c_O averaging 1.6×10^{-6} mass%. Left: Evidence of local initiation of significant oxidation on specimen that was exposed for 10,001 h. Right: Continuous part of oxide layer with non-uniform thickness after exposure for 5011 h.

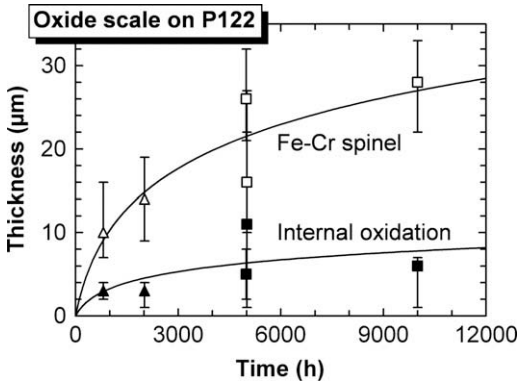

Fig. 4. Thickness of spinel and IOZ as a function of time for the exposure of P122 to oxygen-containing flowing LBE at 550 °C, $v = 2$ m/s and $c_O \approx 1.6 \times 10^{-6}$ mass% with error bars indicating the deviation of the maximum and minimum measured value from the average. Open and solid triangles mark values obtained from a parallel investigation on differently heat-treated P122.

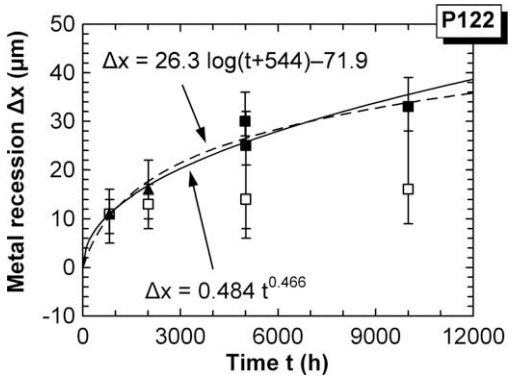

Fig. 5. Metal recession as a function of time for the exposure of P122 to oxygen-containing flowing LBE at 550 °C and $v = 2$ m/s. Solid symbols: constantly high c_O averaging 1.6×10^{-6} mass%, where the triangles mark values obtained from a parallel investigation on differently heat-treated P122. Open squares: varying conditions with respect to the oxygen content, especially temporarily very low c_O. Error bars indicate the deviation of the maximum and minimum measured value from the average.

temporarily very low c_O, together with the equations and average curves following from fitting power and logarithmic rate laws to the data obtained at constantly high c_O. Using these equations for predicting the material degradation after 100,000 h in contact with flowing LBE at 550 °C and $c_O \approx 10^{-6}$ mass% (which implies neglecting a potentially detrimental effect of the slight Cr-depletion of the steel beneath the oxide scale), the logarithmic rate law yields a loss of 60 µm; a more conservative estimate of 103 µm follows from the power rate law (which is approximately parabolic). 60–103 µm is also the range of oxide-scale thickness (spinel plus IOZ) that can be expected after 100,000 h under these conditions, from which 70–80% accounting for spinel may have to be considered with respect to a significant effect on heat-transfer properties. The temporarily very low c_O occurring in the exposure experiments significantly reduced the metal recession/oxide-scale thickness for exposure times $\geqslant$5000 h (Fig. 5).

Besides the "regular" oxidation of P122 described above, two types of exceptional behaviour were observed. In the first case, Cr-depleted stumps formed in a rugged instantaneous steel surface, followed by partial spalling of surrounding Fe–Cr spinel (Fig. 6). According to Wagner [8], such a pronouncedly non-planar surface profile is a consequence of (Cr) diffusion in the steel being the rate-determining step of oxide growth. Partial spalling of the spinel may be promoted by porosity resulting from Fe diffusion

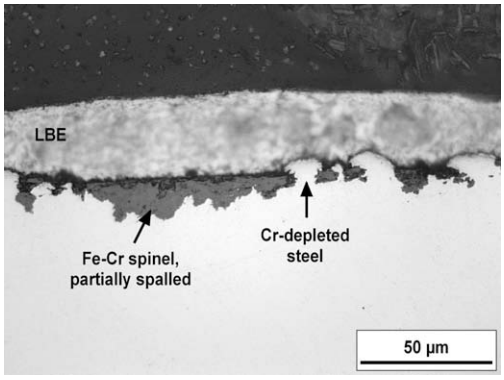

Fig. 6. Pronouncedly non-uniform surface profile and Cr-depleted metallic stumps surrounded by partially spalled spinel on P122 after exposure to LBE at 550 °C, $v = 2$ m/s and $c_O \approx 1.6 \times 10^{-6}$ mass% for 4990 h.

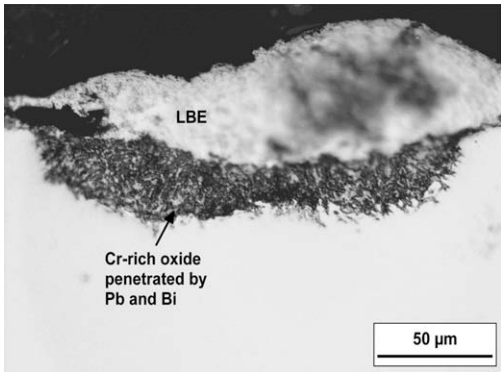

Fig. 7. Liquid–metal assisted corrosion of P122 after exposure to LBE at 550 °C, $v = 2$ m/s and $c_O \approx 1.6 \times 10^{-6}$ mass% for 5011 h.

from the interface with the oxide into the Cr-depleted stumps (maximum Fe activity at this interface) or from inside the spinel towards the spinel surface (minimum Fe activity at interface with the LBE). Cr-depleted stumps and partial spalling of spinel were observed only on specimens that were exposed for 4990 h at constantly high c_O in the interval from 5016 to 10,006 h—both without and after a preceding period of 5016 h under varying conditions, mostly very low c_O—so that these phenomena may arise primarily from the specific history of the oxygen content in the LBE, e.g., the fluctuations between $\sim 10^{-6}$ mass% and higher c_O in the first $\sim$2000 h of this interval (*cf.* Fig. 2). As already mentioned above, sites corresponding to Fig. 6 were neglected when quantifying corrosion. However, there were indications that the local metal recession at such sites may be about 60% higher than following from Fig. 5, most likely depending strongly on the incubation period for spalling of the spinel. The other exception from regular oxidation was observed on the specimen that was exposed for 5011 h at constantly high c_O in the interval from 10,006 to 15,017 h and is characterized by massive ingress of Pb and Bi into the steel (Fig. 7). According to qualitative EDX analyses, the resulting heterogeneous zone contains the constituents of LBE and Cr-rich oxides, while Fe was largely removed, e.g., via diffusion in the liquid–metal phase. At the specific site shown in Fig. 7, the heterogeneous zone was partially eroded by the liquid–metal flow, and the local metal recession approximates twice the average loss by regular oxidation measured for that particular specimen. It should be emphasized that this type of enhanced corrosion was found only once in the examined cross-sections of the specimen that was exposed for 5011 h, and never on the other specimens investigated in this study, especially not on those which experienced a temporarily very low c_O in the LBE. Therefore, a local peculiarity in the steel structure is the likely reason for the occurrence of this phenomenon rather than a considerable susceptibility of P122 to liquid–metal corrosion under the conditions of the experiment. In general, moderate oxidation of P122 predominates, even if the oxygen content temporarily falls in the range of 10^{-9} mass%. However, in the case of all specimens investigated, exposure to flowing LBE started at c_O around 10^{-6} mass% or higher.

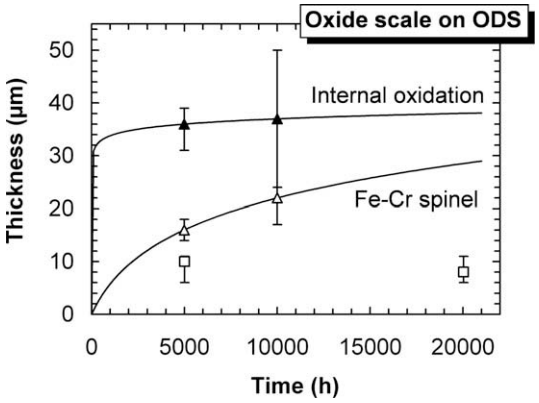

Fig. 9. Thickness of spinel and IOZ as a function of time for the exposure of ODS to oxygen-containing flowing LBE at 550 °C, $v = 2$ m/s and $c_O \approx 1.6 \times 10^{-6}$ mass% with error bars indicating the deviation of the maximum and minimum measured value from the average. Open and solid triangles mark values obtained from specimens the exposure of which started with $c_O > 10^{-6}$ mass%. The open squares symbolize the spinel thickness on specimens the exposure of which started with $c_O \leqslant 10^{-6}$ mass% (no internal oxidation in this case).

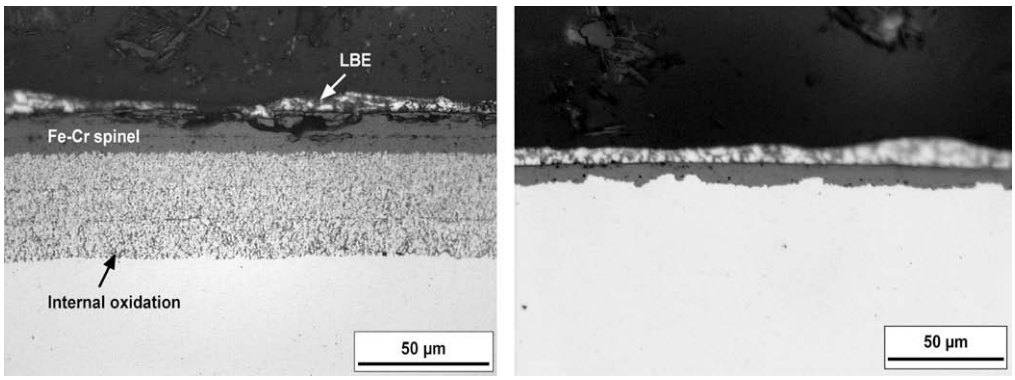

Fig. 8. Oxide scales observed on ODS after exposure for about 5000 h to flowing LBE at 550 °C and constantly high c_O averaging 1.6×10^{-6} mass%. Left: Pronounced internal oxidation after exposure for 4990 h that started with $c_O > 10^{-6}$ mass%. Right: Comparatively thin, single spinel layer formed in the course of exposure for 5011 h that started with $c_O \leqslant 10^{-6}$ mass%.

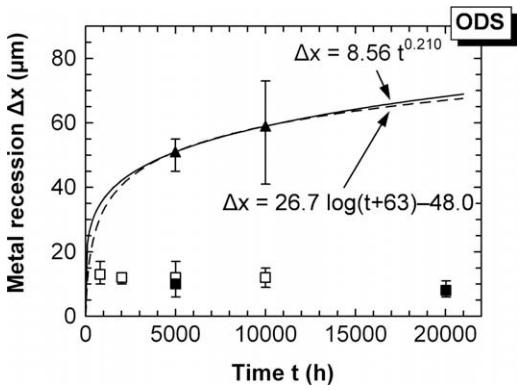

Fig. 10. Metal recession as a function of time for the exposure of ODS to oxygen-containing flowing LBE at 550 °C and v = 2 m/s. Solid symbols: constantly high c_O averaging 1.6×10^{-6} mass%, where the triangles mark values obtained from specimens the exposure of which started with $c_O > 10^{-6}$ mass%. Open squares: varying conditions with respect to the oxygen content, especially temporarily very low c_O. Error bars indicate the deviation of the maximum and minimum measured value from the average.

3.2. 9Cr–2W ODS steel

When exposed to oxygen-containing flowing LBE at 550 °C and v = 2 m/s, ODS forms a continuous layer of Cr-deficient Fe–Cr spinel (following from the combined results of XRD and EPMA analyses) and, in general, a more or less pronounced IOZ consisting of Cr-rich oxide particles finely dispersed in the Cr-depleted steel matrix (Fig. 8). Comparing specimens that were exposed under nominally the same conditions but in different exposure intervals, the progress of oxidation—especially of internal oxidation—can considerably vary, indicating an exceptionally high sensitivity of the performance of ODS on the history of the exposure, i.e., the specific development of c_O with time. In this regard, the conditions in the beginning of the exposure period, e.g., the first 1000–2000 h, seem to be more decisive than the following 8000–18,000 h. This finding is corroborated by Figs. 8 and 9, showing moderate spinel formation and substantial internal oxidation for specimens that were exposed for 4990 and 10,001 h, respectively, at constantly high c_O, starting with c_O fluctuating significantly between 10^{-6} mass% and higher values (Fig. 8, left and triangles in Fig. 9; *cf.* Fig. 2 and Table 2). After exposures for 5011 and 20,039 h that started with c_O around 10^{-6} mass% and lower, only a relatively thin spinel layer with non-uniform thickness formed and internal oxidation is completely missing (Fig. 8, right and squares in Fig. 9). In the latter case, qualitative EDX analyses indicate an enrichment of Cr in the relatively thin spinel layer at the spinel/steel interface. Local enrichment of Cr in the spinel and decreased internal oxidation were also observed on the specimens that experienced longer periods of very low c_O. Under conditions favouring internal oxidation, a thin, piecewise continuous layer of precipitated Cr-rich oxide occasionally formed at the IOZ/steel interface. In general, such piecewise continuous layers did not have a long-lasting effect on the progress of internal oxidation, but can explain the increase with time of local deviations from the average thickness of the IOZ (solid triangles in Fig. 9). Besides spinel formation and internal oxidation, the exposure to oxygen-containing LBE may result in Cr-depletion of the steel at the oxide scale/steel interface, which is potentially more significant—and accompanied by the transformation of the martensitic steel into ferrite—in the absence of an IOZ (beneath a single spinel layer enriched in Cr) or where internal oxidation established a piecewise continuous layer of Cr-rich oxide at the IOZ/steel interface. However, Cr-depletion was not evident from EDX analyses on the specimen that was exposed for 20,039 h under conditions favouring a thin single spinel layer.

The metal recession as a function of the exposure time determined from the sum of the thicknesses of the spinel layer and the IOZ (if present) are depicted in Fig. 10. Accordingly, the metal recession for specimens that experienced either comparatively long-lasting deviations of c_O towards very low values or constantly high c_O starting with $\leqslant 10^{-6}$ mass% is in the range of 10 μm and does not significantly change for exposure times between ~800 and 20,000 h, which most likely is a favourable effect of the accumulation of Cr in the spinel layer at the interface with the steel. If substantial internal oxidation occurs, the metal recession is in the range of 60 μm after 10,000 h. Fitting logarithmic and power rate laws to the sparse data for these conditions resulted in the

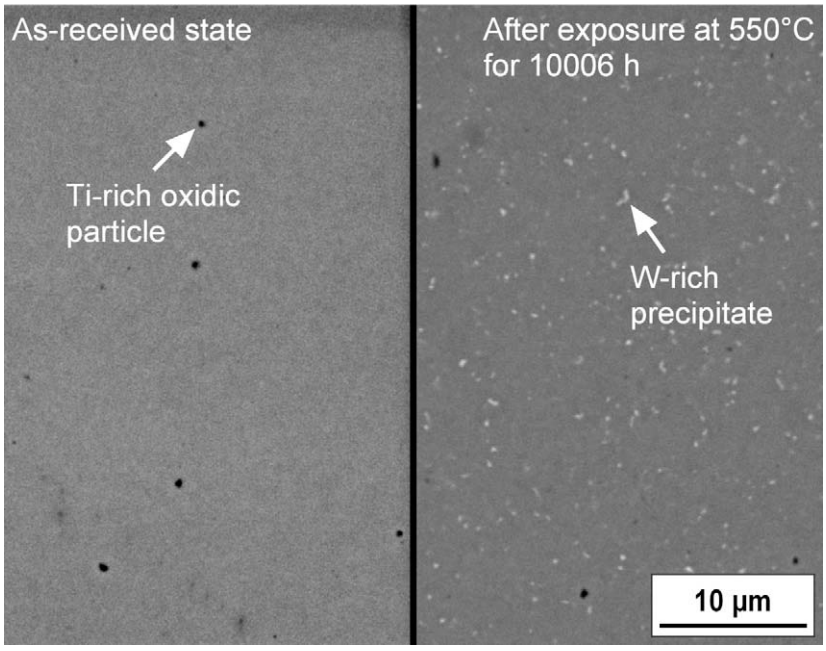

Fig. 11. Electron-optical micrographs of polished ODS in the as-received condition (left) and after exposure for 10,006 h at 550 °C in the CORRIDA loop (right).

equations shown in Fig. 10 which predict a material loss of 85 (logarithmic) and 96 μm (power law) after 100,000 h. However, this range may only be a rough estimate, as only the minimum number of data points necessary for extrapolation was available. The part of the metal recession after 100,000 h accounting for spinel formation is estimated at 50–65%.

Irrespective of whether c_O was constantly around 10^{-6} mass% or varied considerably between higher and much lower values, major exceptions from the performance of ODS described above were not observed. Especially, indications that the oxide scale formed on ODS could not prevent the direct contact between the liquid metal and the steel were not found in this study. A minor deviation observed after exposure for 2018 h under varying conditions with respect to c_O was the local presence of a Fe_3O_4 layer with non-uniform thickness on top of the spinel.

In addition to oxidation, the exposure at 550 °C gave rise to the precipitation of W-rich particles appearing as bright spots in electron-optical micrographs (Fig. 11). According to a rough qualitative assessment of the density and size of these particles after different exposure times, the precipitation process was largely finished after 5000 h. The post-test examinations did not provide evidence for a decisive influence of the W-rich precipitates on the oxidation of ODS, but an impact on the long-term mechanical properties can be expected.

4. Conclusions

P122 and the investigated 9Cr–2W ODS steel show a promising long-term performance in oxygen-containing flowing LBE at 550 °C, $v = 2$ m/s and constantly high c_O averaging 1.6×10^{-6} mass% for exposure times up to 10,000 and 20,000 h, respectively. Neglecting a slight Cr-depletion beneath the formed oxide scales, the expected material loss (metal recession) after 100,000 h is in the range of 100 μm or lower for both steels. With respect to a detrimental effect of oxidation on heat-transfer properties, only a compact oxide layer (Cr-deficient Fe–Cr spinel) accounting for 70–80% (P122) or 50–65% (ODS) of the total metal recession may have to be considered. However, partial spalling of the oxide layer, observed as an exception on specimens of P122, can at least locally increase the metal recession, the more pronounced the earlier and the more often spalling occurs. In the case of ODS—the performance of which proved to be especially sensitive to short-term fluctuations in the oxygen content of the LBE—metal recession apparently remains constantly in the range of 10 μm for exposure times up to 20,000 h if the conditions favour the accumulation of Cr at the oxide/steel interface in a single layer spinel scale instead of substantial internal oxidation of the steel. In this regard, c_O should be around 10^{-6} mass% or less and, more importantly, temporarily higher c_O has to be prevented at least for the first 1000–2000 h. Comparatively long-lasting excursions of c_O down to $\sim 10^{-9}$ mass% significantly reduce the metal recession caused by oxidation for both steels without any indication that the oxide scale formed cannot protect the steel from direct contact with LBE. The only site where this protection was imperfect was found on a specimen of P122 after exposure for ~5000 h at constantly high c_O around 10^{-6} mass%, which most likely resulted from a local peculiarity in the steel microstructure and underlines the need for high-quality/purity material rather than questioning the general applicability in oxygen-containing LBE.

Considering the findings on the influence of variations of the oxygen content, $c_O \approx 10^{-6}$ mass% is not optimum with respect to slow oxidation concurring with the protection of the steel from direct contact with LBE, and, in the case of both P122 and ODS, can probably be at least one order of magnitude lower (corresponding to $a_{PbO} \approx 10^{-4}$). For ODS, substantial internal oxidation would be prevented, and for P122, the initially present thin Cr-rich oxide scale might be stabilized, providing a considerable gain in oxidation resistance. However, especially the latter needs to be proven by additional experiments.

Acknowledgements

The presented study was part of a joint project of the former Japan Nuclear Cycle Development Institute and the Karlsruhe Research Centre. Special thanks go to O. Wedemeyer, Z. Voß and J. Novotny for preparing the exposure experiments and operating the CORRIDA loop.

References

[1] L. Soler Crespo, in: Handbook on Lead–Bismuth Eutectic Alloy and Lead Properties, Materials Compatibility, Thermal Hydraulics and Technologies, NEA-Report No. 6195, OECD, 2007, Chapter 6, pp. 231–274.
[2] J. Zhang, N. Li, J. Nucl. Mater. 373 (2008) 351.
[3] S. Ukai, M. Fujiwara, J. Nucl. Mater. 307–311 (2002) 749.
[4] C. Schroer, Z. Voß, O. Wedemeyer, J. Novotny, J. Konys, J. Nucl. Mater. 356 (2006) 189.
[5] C. Schroer, J. Konys, Physical Chemistry of Corrosion and Oxygen Control in Liquid Lead and Lead–Bismuth Eutectic, Report FZKA 7364, Forschungszentrum Karlsruhe, Germany, 2007. <http://bibliothek.fzk.de/zb/berichte/FZKA7364.pdf>.
[6] C. Schroer, Z. Voß, J. Novotny, J. Konys, Quantification of the Degradation of Steels Exposed to Liquid Lead–Bismuth Eutectic, Report FZKA 7224, Forschungszentrum Karlsruhe, Germany, 2006. <http://bibliothek.fzk.de/zb/berichte/FZKA7224.pdf>.
[7] P. Kofstad, High Temperature Corrosion, Elsevier Applied Science Publishers Ltd., 1988. pp. 15–22.
[8] C. Wagner, J. Electrochem. Soc. 103 (1956) 571.